

The Flattening of Dendrimers from Solutions onto Charged Surfaces: Supplemental Information

P. M. Welch,^{*} C. F. Welch, and N. J. Henson

*Theoretical and Materials Science and Technology Divisions, Los Alamos National Laboratory,
Los Alamos, New Mexico 87544*

E-mail: PWelch@lanl.gov

Estimating the Effective Step Length l_1

The effective step length is given by the cubic root of the equation below, mapping the observed squared radius of gyration of the dendrimer Rg^2 to l_1 .

$$Rg^2 = l_1 \frac{M_1(L_B, G)}{(3L_B[2^G - 1])^2} + l_1^2 \frac{M_2(L_B, G)}{(3L_B[2^G - 1])^2} + l_1^3 \frac{M_3(L_B, G)}{(3L_B[2^G - 1])^2} \quad (1)$$

The three functions of contour length between branch points L_B and generation of growth G are given by, $M_1(L_B, G) = L_B^3(3\{-1 + 6 * 2^G + [3G - 5]2^{2G}\} - 4.5 * 2^G(2^G - 1) + 3.5(2^G - 1))$, $M_2(L_B, G) = L_B^2(-(2^G - 1) + 4.5 * 2^G(2^G - 1) - 3.5(2^G - 1))$ and $M_3(L_B, G) = L_B(2^G - 1)$.

Further details on the derivation and assumptions employed in arriving at this expression may be found in reference 25 of the main paper.

Simulation Details

The thermal energy kT sets the energy scale for the simulation and was set to a raw value of 1.0. At this value of kT , the implicit solvent acts as a “good solvent” for the dendrimers. The pairwise interactions between particles separated by a distance $r_{i,j}$, reflecting both excluded volume

^{*}To whom correspondence should be addressed

and short-ranged attractions, were modeled by the Morse potential, $U_M = U_0((1 - \text{Exp}[-\alpha(r_{i,j} - r_{min}))])^2 - 1)$. Here, U_0 is the well-depth, the effective range of the potential varies with α , and r_{min} dictates the location of the minimum of the potential. All particles interacted with a value of $U_0/kT = 1.0$ and a range parameter of $\alpha l_w = 24$, while the potential minimum was set such that $r_{min}/l_w = 0.8$.

The FENE potential, $U_F = -\frac{Kr_0^2}{2} \ln[1 - (\frac{l-l_0}{r_0})^2]$, captures the energy due to bonds of length l . The equilibrium step length l_0 for the dendrimer was set such that $l_0/l_w = 0.7$, reflecting the typical distance between branch points within PPI dendrimer. The spring constant K and the half-width of the potential r_0 were set such that $Kl_w^2/kT = 2000$ and $r_0/l_w = 0.3$. These parameter values, in combination with the value of r_{min} described above, prevent bond crossing in the mobile molecules.

The electrostatics were modeled with the Coulombic potential, $U_C = \frac{kTl_w q_i q_j}{\epsilon r_{i,j}}$, truncated at a cutoff distance r_c . Here, q_i and q_j are the charges on particles i and j (± 1 for the dendrimer segments and counter ions; varying for the electrodes). The dielectric constant ϵ within these units is set to one for a water-like solvent. The potential was truncated at $r_c/l_w = 5$ in all scenarios.

For clarity of notation, Figure S1 provides a schematic of a generation 2 model used in our simulations. The pairwise interactions described above act between all blue beads within the prescribed cutoffs. The red cylinders represent the bonds maintained by the FENE potential.

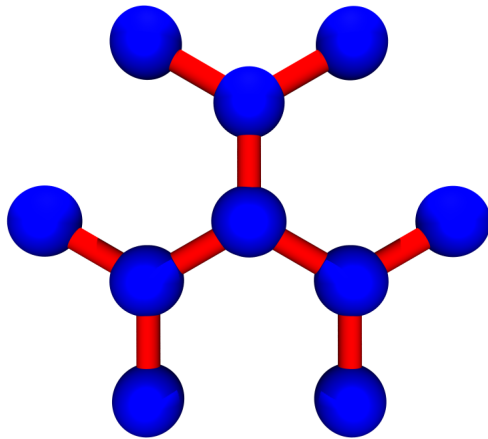


Figure S1: A schematic of the model dendrimer used herein. A $G = 2$ molecule is illustrated.

All simulations were carried out using the LAMMPS molecular dynamics code using the Langevin thermostat, a unit frictional coefficient, and a time step $\Delta t = 0.004$. The simulations were carried out in two stages. During the first stage, the electrodes are neutral and the electrolyte solutions are allowed to equilibrate for 10 to 50 million time steps. Next, the electrode particles are uniformly assigned their respective charges and the electrolyte evolves in the field presented by the electrodes for 6 - 90 million time steps. Coordinates were saved every 250 thousand time steps in both stages.

Ion Distribution and Net Charge Densities

For comparison, Fig. S2 herein presents $P(z)$ for the ion segments in the corresponding set of simulations presented in Fig. 2 of the main article. Note that the ion distributions largely mirror those of the dendrimers.

In order to illustrate more clearly the charge distribution within a typical simulation, Figure S3 presents the segment density (number of segments per volume within a slice) for a $G = 5$ dendrimer at $2c^*$ sandwiched between two electrodes with $\sigma l_w^2 = 1.0$, as well as the corresponding net charge density. Near the positive electrode (left side of graph), the dendrimer density rises sharply and the net charge becomes negative. Conversely, the negative electrode (right side) shows an increase in net charge as the result of accumulation of counter ions.

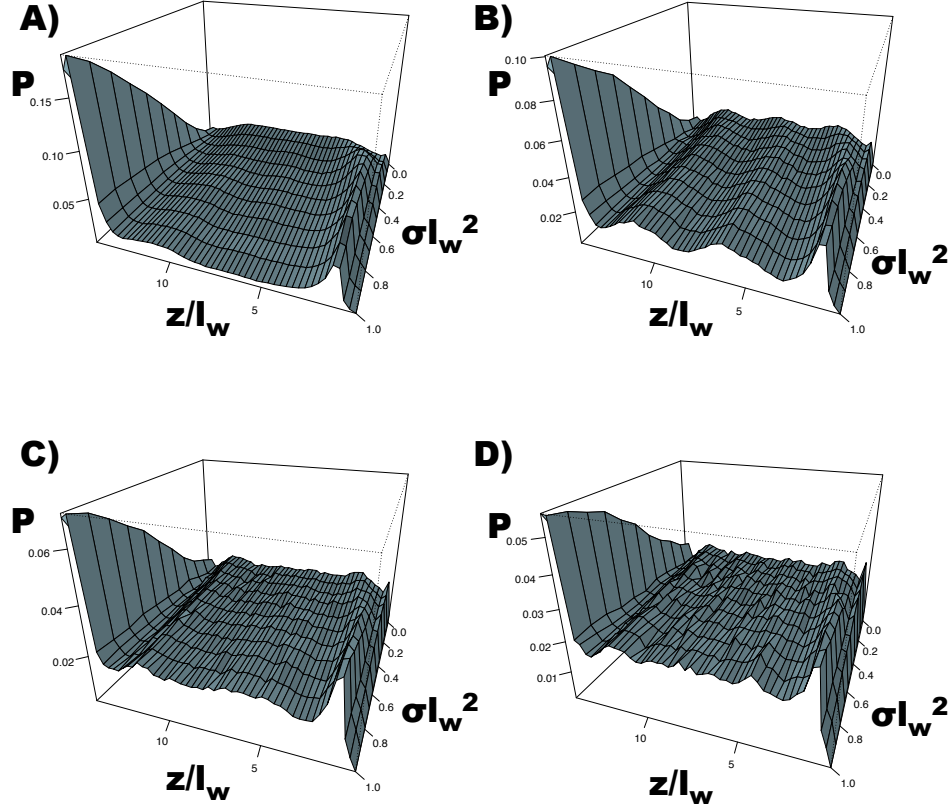


Figure S2: The probability P of finding a model ion segment along the perpendicular axis between the two electrodes as a function of reduced surface charge density σl_w^2 . Data corresponding to the simulations presented in Fig. 2 of the main article are presented. Plots for $G = 3$ and concentrations A) $0.5c^*$, B) c^* , C) $1.5c^*$, and D) $2c^*$ are shown.

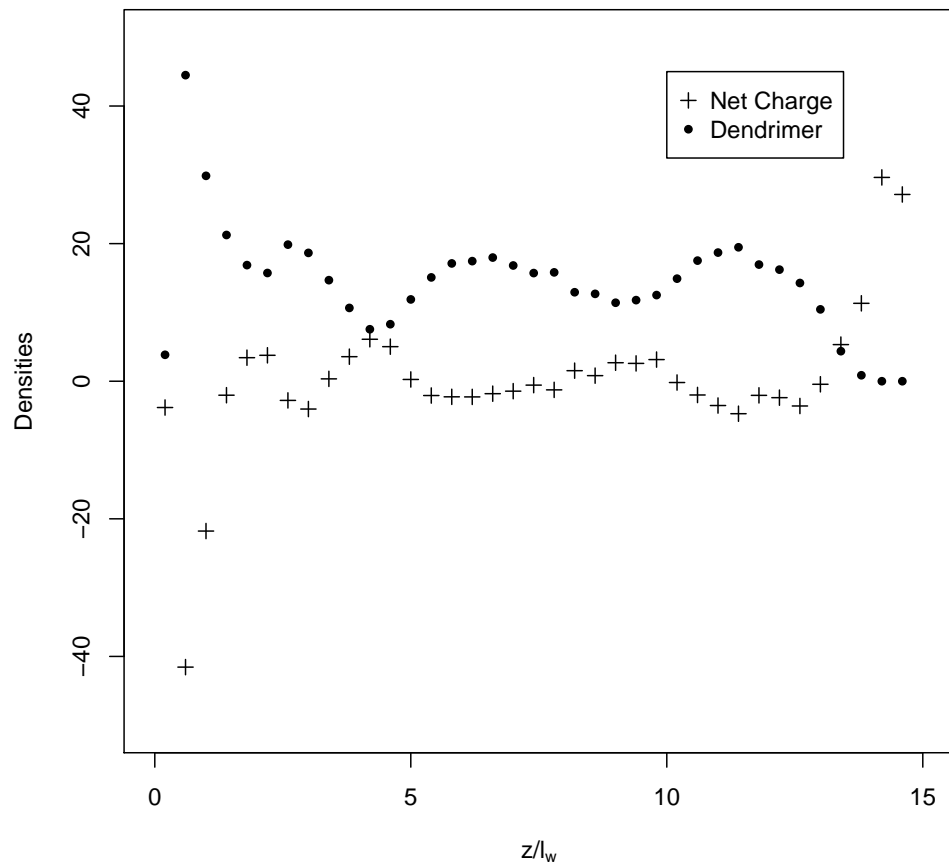


Figure S3: The dendrimer segment density and net charge density for a $G = 5$, $2c^*$, $\sigma l_w^2 = 1.0$ simulation.